PROCEEDINGS OF SPIE

SPIEDigitalLibrary.org/conference-proceedings-of-spie

3D registration of depth data of porous surface coatings based on 3D phase correlation and the trimmed ICP algorithm

Nina Loftfield, Markus Kästner, Eduard Reithmeier

Nina Loftfield, Markus Kästner, Eduard Reithmeier, "3D registration of depth data of porous surface coatings based on 3D phase correlation and the trimmed ICP algorithm," Proc. SPIE 10333, Optical Methods for Inspection, Characterization, and Imaging of Biomaterials III, 1033310 (26 June 2017); doi: 10.1117/12.2269781

SPIE.

Event: SPIE Optical Metrology, 2017, Munich, Germany

3D registration of depth data of porous surface coatings based on 3D phase correlation and the Trimmed ICP algorithm

Nina Loftfield[a], Markus Kästner[a], and Eduard Reithmeier[a]

[a]Leibniz Universität Hannover, Institute of Measurement and Automatic Control, Nienburgerstrasse 17, 30167 Hannover, Germany

ABSTRACT

A critical factor of endoprostheses is the quality of the tribological pairing. The objective of this research project is to manufacture stochastically porous aluminum oxide surface coatings with high wear resistance and an active friction minimization. There are many experimental and computational techniques from mercury porosimetry to imaging methods for studying porous materials, however, the characterization of disordered pore networks is still a great challenge. To meet this challenge it is striven to gain a three dimensional high resolution reconstruction of the surface. In this work, the reconstruction is approached by repeatedly milling down the surface by a fixed decrement while measuring each layer using a confocal laser scanning microscope (CLSM). The so acquired depth data of the successive layers is then registered pairwise. Within this work a direct registration approach is deployed and implemented in two steps, a coarse and a fine alignment. The coarse alignment of the depth data is limited to a translational shift which occurs in horizontal direction due to placing the sample in turns under the CLSM and the milling machine and in vertical direction due to the milling process itself. The shift is determined by an approach utilizing 3D phase correlation. The fine alignment is implemented by the Trimmed Iterative Closest Point algorithm, matching the most likely common pixels roughly specified by an estimated overlap rate. With the presented two-step approach a proper 3D registration of the successive depth data of the layer is obtained.

Keywords: 3D registration, porous surface, 3D phase correlation, TrICP

1. INTRODUCTION

A surface represents the interface of two components and a lot of applications depend on the surface properties.[1] Considering endoprostheses, a critical factor is the quality of the tribological pairing which, in turn, is strongly influenced by the surface texture and microstructure. In this work stochastically porous aluminum oxide (Al_2O_3) surface coatings, manufactured by a thermal spraying process, are investigated. The objective of this research project is to manufacture surfaces with high wear resistance and an active friction minimization. This is approached by embedding a channel system beneath the surface, which is to serve as a reservoir for lubricants. Due to the porosity of the surface layer, which is affected by the parameters of the thermal spraying process, the lubricant is to pass through the coating and escapes on the top level. In porous media the fluid flow is strongly dependent on morphological and topological parameteres like the pore size and shape and the pore connectivity.[2] Therefore, the characterization of the porous microstructure is of importance and serves a better understanding of the material properties and the manufacturing process.

This work focuses on the examination of the porous network of the surface coating. Although, there are many experimental and computational techniques known from mercury porosimetry to imaging methods for studying porous materials, the characterization of disordered pore networks is still a great challenge. The digital reconstruction of porous media is accomplished either by modeling or direct 3D measuring approaches. Modeling is based on stochastic methods, reconstructing the porouse media on the basis of one or several thin 2D slices or process-based methods, imitating the physical processes structuring the porous media.[2] Two direct, straight

Further author information:
E-mail: nina.loftfield@imr.uni-hannover.de

Optical Methods for Inspection, Characterization, and Imaging of Biomaterials III, edited by Pietro Ferraro, Simonetta Grilli, Monika Ritsch-Marte, Christoph K. Hitzenberger, Proc. of SPIE Vol. 10333, 1033310
 · doi: 10.1117/12.2269781

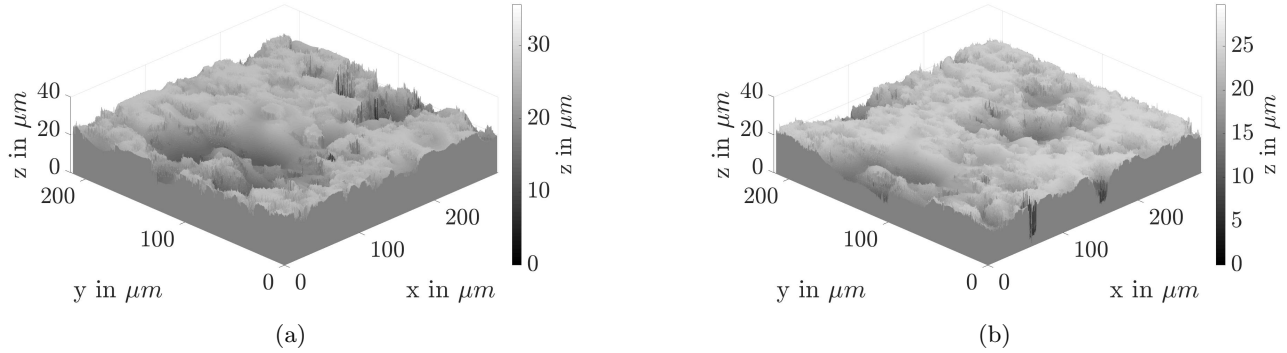

Figure 1: Raw measurement data of two sequential subsurfaces (a) and (b).

forward approaches of measuring the structure in 3D, e.g., are scanning the media with a 3D computer tomograph or using focused ion beam (FIB) combined with scanning electron microscopy (SEM). For example, Drach et al. use X-ray microtompgraphy data to characterize volume, shape and orientation distribution of pores in chemical vapor infiltrated carbon/carbon composites.[3] Further, Balach et al.[4] and Joos et al.[5] use the combination of FIB and SEM for the 3D reconstruction of porous media. In the work of Balach et al. mesoporous carbon with tailored pore size is reconstructed and characterized whereas Joos et al. study the porous network of electrodes. In both works, however, the difficulty of finding the correct threshold to segement the pore structure from the solid material is adressed.[4,5]

We approach the challenge of gaining a three dimensional high resolution reconstruction of the coating by repeatedly milling the surface with a fixed decrement with fly cutting milling while measuring each subsurface using a confocal laser scanning microscope (CLSM), which provides depth data of each layer. This way, in addition to the structure of pores apparent on the layers' surface, the structure of embedded pores can be characterized, further, enabling the distinction of the efficient porosity and inefficient porosity. The advantage of measuring the structure with a CLSM is the direct measurement of the pores boundaries. The structure boundary is independent on an evaluated threshold. However, to accomplish a later 3D reconstruction of the pore network of the porous Al_2O_3 coating off the depth data, in a first step the subsurfaces need to be registered precisely, which is discussed in this paper.

2. MATERIAL AND METHODS

2.1 Ceramic Layers

The investigated surfaces are comprised of porous Al_2O_3 layers with a nominal planar surface. The layers are manufactured by a thermal spraying process and are subsequently polished. The porosity is influenced by the process parameters and the material composition. Information about the volume structure is gained by milling the layer with a step size of approximately $2\mu m$. The orientation of the milling direction is in line with the height information (z-direction). The surface itself is spanned in the x-y-direction. The used CLSM is the VK-X200 from Keyence. The milled surfaces will be referred to as subsurfaces. Each of the subsurfaces is measured individually. All data shown in this work are acquired with a $50x$ magnification lens with a NA $= 0.95$, respectively with a lateral pixel resolution of $0.277\mu m$. Fig. 1 shows two sets of raw measurement data of two sequential measurements. It can be observed that the topography changes in between the milling steps due to the porosity and the measurement field is shifted horizontally. Thus the challenge appears of aligning the sequential data.

2.2 Preprocessing

The preprocessing covers two issues, noise suppression and tilt correction. Both steps have to be applied to each milled subsurface individually. Fig. 2 shows the measurements data of a subsurface before and after preprocessing. The topography data holds less noise and the main plane is transformed so that the reference

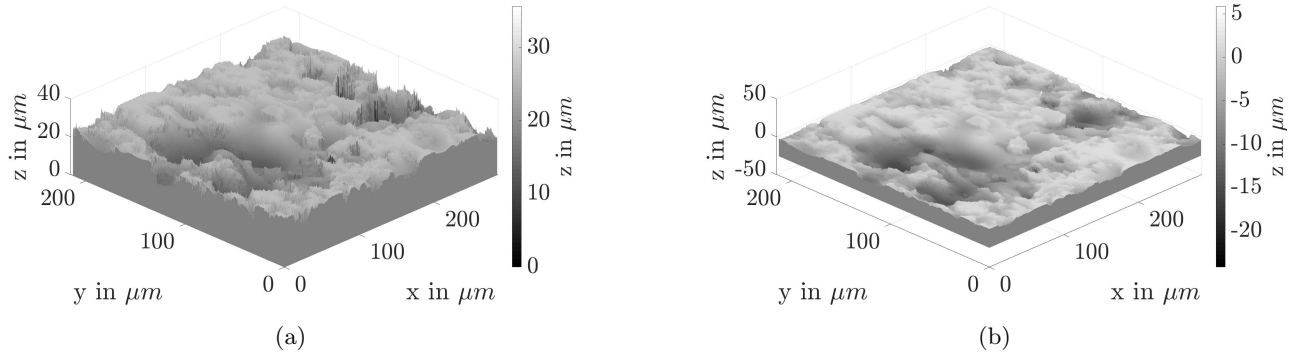

Figure 2: Raw data (a) and preprocessed data (b).

plane is at zero level. Noise suppression is covered by 3D Gaussian filtering. The used kernel size of the Gaussian filter depends on the resolution of the acquired data according to the DIN Norm: EN ISO: 25178 Geometric Product Specifications (GPS) Surface texture: areal.[6] Data with a lateral pixel resolution of dx = dy = $0.277\mu m$ is, therefore, filtered with a cutoff frequency in x- and y-direction of $\lambda_{\mathrm{xc}} = \lambda_{\mathrm{yc}} = 0.8\mu m$.

The tilt correction is implemented by a robust plane fit based on a total least square approach. To minimize the influence of outliers and structure components like pores a weighted least square algorithm is implemented. For further information on the use of a robust plane fit for planar surface alignment in the field of application of surface characterization, see Hao.[7]

2.3 3D Registration

Image registration is an active research area and can in general be categorized in two approaches: direct (appearance) and feature based techniques. With the direct approach the transformation is evaluated to match most pixels best according to a cost function. Whereas, within feature based techniques, the transformation is determined on the basis of detected and matched features in both datasets. Within this work a direct registration approach is implemented in two steps, a coarse and a fine alignment. The coarse alignment of the depth data is limited to a translational shift which occurs in horizontal direction due to placing the sample in turns under the CLSM and the milling machine and in vertical direction due to the milling process itself. The shift is determined by an approach utilizing 3D phase correlation, which has a high robustness regarding the discontinuity of the microstructures in each layer. Based on the coarse alignment in three directions, the successive depth data is further processed and narrowed down to the most likely common pixels which serves the fine alignment. The fine alignment is implemented by the Iterative Closest Point (ICP) algorithm, matching the data by minimizing the mean square error point to point distance between the two datasets. Because the subsequent datasets only overlap in regions deeper than the milling step size and it is not to be guaranteed that all matched data points are outlier-free the Trimmed ICP (TrICP) presented by Chetverikov et al.[8] rather than the original ICP algorithm is used. The TrICP estimates the rigid transformation matrix according to a given overlap rate and takes only the trimmed point pairs, the least trimmed squares, respectively, into account. The subsurfaces are than registered pairwise successively, first by the coarse and later by the fine alignment.

2.3.1 3D phase correlation

Phase correlation is an established approach in image registration to estimate the relative translational shift between two datasets. Phase correlation is based on the frequency-domain representation of the data. A shift in the spatial domain of two datasets results in a linear phase difference in the frequency-domain of the Fourier Transforms (FT). This applies to all dimensions independently. In case of 3D phase correlation this means that the shift in all three spatial directions $(\Delta x, \Delta y, \Delta z)$ is determined between two volumes $V_1(x, y, z)$ and $V_2(x, y, z)$:

$$(\Delta x, \Delta y, \Delta z) = \mathrm{3DPhaseCorr}(V_1(x, y, z), V_2(x, y, z)). \tag{1}$$

Before aligning the topographies, the topographies' height data is converted into a 3D volume representation. This is implemented by an interpretation of the height value of the surface as the z-coordinate. Primarily to transforming the volume data in the frequency domain by applying the 3D Fast Fourier Transformation (FFT), the volume data is filtered by the Hanning window function to avoid edge effects and reducing the effects of noise when transforming into the frequency-domain. With the FTs, $F_{1_{x,y,z}} = FFT(V_1(x,y,z))$ and $F_{2_{x,y,z}} = FFT(V_2(x,y,z))$, the normalized cross power spectrum, denoted $F_{3_{x,y,z}}$, is given by

$$F_{3_{x,y,z}} = \frac{F_{1_{x,y,z}} \odot F^*{}_{2_{x,y,z}}}{|F_{1_{x,y,z}} \odot F^*{}_{2_{x,y,z}}|}, \tag{2}$$

where * denotes the complex conjugate, $\odot$ the element wise multiplication and $|x|$ the magnitude function. The inverse of the normalized cross power $FFT^{-1}(F_{3_{x,y,z}})$ gives the phase correlation volume $V_3(x,y,z)$. The peak value in $V_3(x,y,z)$ corresponds to the relative shift:

$$(\Delta x, \Delta y, \Delta z) = -[\arg\max_{(x,y,z)}(V_3(x,y,z))]. \tag{3}$$

Beyond the translational shift, other transformation factors like scaling and rotation can be evaluated using the 3D phase correlation, for further information on this see Lincoln and Gonzalez.[9] In this work, however, there is no scaling change throughout the aligned volumes that needs to be considered and the rotation in between to volumes is negligibly small and, if present, will be covered by the fine alignment.

2.3.2 Trimmed ICP

The ICP algorithm, first introduced by Chen and Medioni[10] and Besl and McKay,[11] is a standard tool in the registration of two roughly preregistred point clouds, which can be of any 3D shape or surfaces. A set of data points $\mathcal{P} = \{p_i\}_1^{N_p}$ is transformed (combination of translation and rotation) $\mathcal{P}(\mathrm{R},\mathrm{t}) = \{p_i(\mathrm{R},\mathrm{t})\}_1^{N_p}$ to match a set of model points $\mathcal{M} = \{m_i\}_1^{N_m}$. The transformation operates interatively to minimize an error function, specified by the mean-square distance between the two point sets. Therefore, the distance from each data point $p_i(R,t)$ to the closest point in the model point set $\mathcal{M}$ is defined:

$$m_{cl}(i,R,t) = \arg\min_{m\in\mathcal{M}} ||m - p_i(R,t)||, \tag{4}$$

$$m_i(R,t) = ||m_{cl}(i,R,t) - p_i(R,t)||. \tag{5}$$

Over the past decades many different variants of the ICP have come up, for an overview of most common variants see Rusinkiewicz and Levoy.[12] In this work a modified version, the Trimmed ICP (TrICP) algorithm by Chetverikov et al.,[8] is used. The TrICP algorithm takes into account that the datasets only have a specific overlap rate and that the matched data points are not outlier-free. The transform is estimated according to the overlap rate ξ of both datasets. Therefore, only the trimmed point pairs, the least trimmed squares, respectively, are considered for the matching process, respectivly the number of matched points decreases to $N_{po} = \xi \cdot N_p$. Hence, the standard ICP can be considered a special case of the TrICP with an overlap rate $\xi = 100\%$. According to Chetverikov, the TrICP performs well even with a overlap rate smaller 50% and is robust to erroneous measurements and shape defects.[8]

One drawback, however, is the necessity of knowing the overlap rate ξ beforehand. We estimate the overlap based on the coarse alignment. The number of points of the successive point sets N_m and N_p are of same size, therefore, the overlap rate is determined by the intersection of $\mathcal{P}$ and $\mathcal{M}$ proportionally to the overall point set of one dataset:

$$\xi = \frac{\mathcal{P} \cap \mathcal{M}}{\mathcal{M}}. \tag{6}$$

The intersection is determined by cutting the point set $\mathcal{M}$ vertically according to the shift in z-direction, meaning cutting out points above Δz and horizontally according to $\Delta x, \Delta y$. Fig. 3c illustrates the correspondent point mask of a surface (see Fig. 3a), with white pixels representing pixels most likely to be found in the successive subsurface (see Fig. 3b).

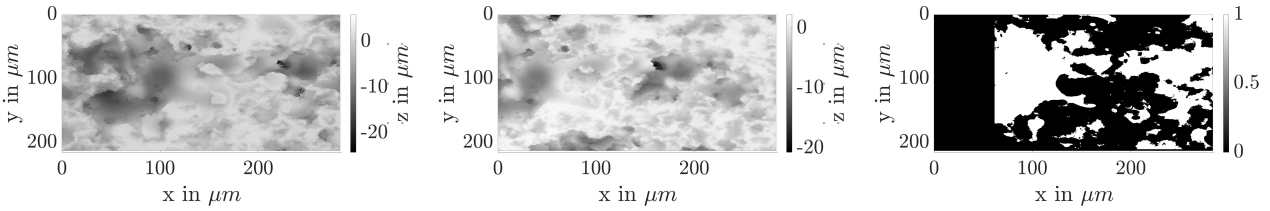

(a) (b) (c)

Figure 3: Estimation of the overlap rate ξ, the percentage of common pixel in the upper (a) and lower (b) subsurface. The mask (c) shows the region of the most likely common pixels (illustrated in white).

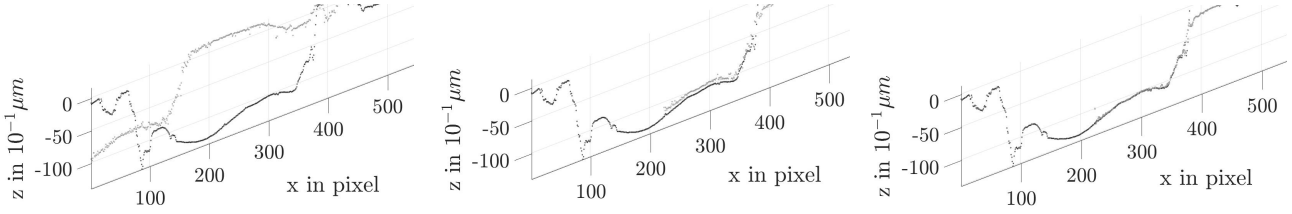

(a) (b) (c)

Figure 4: Profile of not algined surface data (a), after the coarse alignment (b) and after the fine alignment (c).

3. EXPERIMENTAL RESULTS

The results of the registration process are considered separately for the coarse and the fine alignment. The result of the coarse registration is illustrated exemplary in Fig. 4b. For illustration purposes profiles rather than the areal data is shown. However, for all illustrated results the registration was processed on the basis of areal data. It can be seen that the unregistered datasets (see Fig. 4a) are aligned both vertically and horizontally, a good preregistration is achieved. For the coarse alignment, the translational shift in between the measurements within a series of measurements consisting of ten subsurfaces averaged in x-direction: $-0.22 \pm 31.33\mu m$, in y-direction: $0.31 \pm 20.49\mu m$ and in z-direction: $-1.69 \pm 1.18\mu m$. This shows, that the milling process is not as accurate as proposed. However, even with an imprecise previous knowledge of how large the shift in between the measurements is and also with high lateral shifts a good matching is performed. For the successive fine alignment of the same dataset of ten subsurfaces an overlap rate of $\xi = 45 \pm 16\%$ was determined. The translational shifts in between the measurements within the same series of measurements as for the coarse alignment averaged in x-direction $0.01 \pm 0.32\mu m$, in y-direction $0.02 \pm 0.30\mu m$ and in z-direction $0.25 \pm 0.75\mu m$. The rotational shift around the x-axis was $-0.0021 \pm 0.0206°$, around the y-axis $0.0019 \pm 0.0179°$ and around the z-axis $-0.0002 \pm 0.0003°$. As stated, the rotational shift is negligibly small. Fig. 4c illustrates the result of the subsequent fine alignment. In the region of the profile course of the pore the improvement of the registration by the fine alignment is best observable.

Fig. 5a shows the registration result of two subsequent subsurfaces with a high lateral deviation. For illustration purposes, once again, the profiles are depicted, here in x-, y- and z-direction (see Fig. 5b-5d). The height data is matched well in the pore regions observable in both topographies' height data. For the profiles in x- and y-direction, again the results are best shown in the profile course of the pore area. The same structure is measured and aligned accordingly in this regions. For the z-profile, or isolines, the pores' contours fit properly. The occurring difference of the topographies due to the milling process of the porous structure can be well seen in Fig. 5c. The upper and lower course of profile of the subsurfaces vary. These regions are to be left out in the matching process.

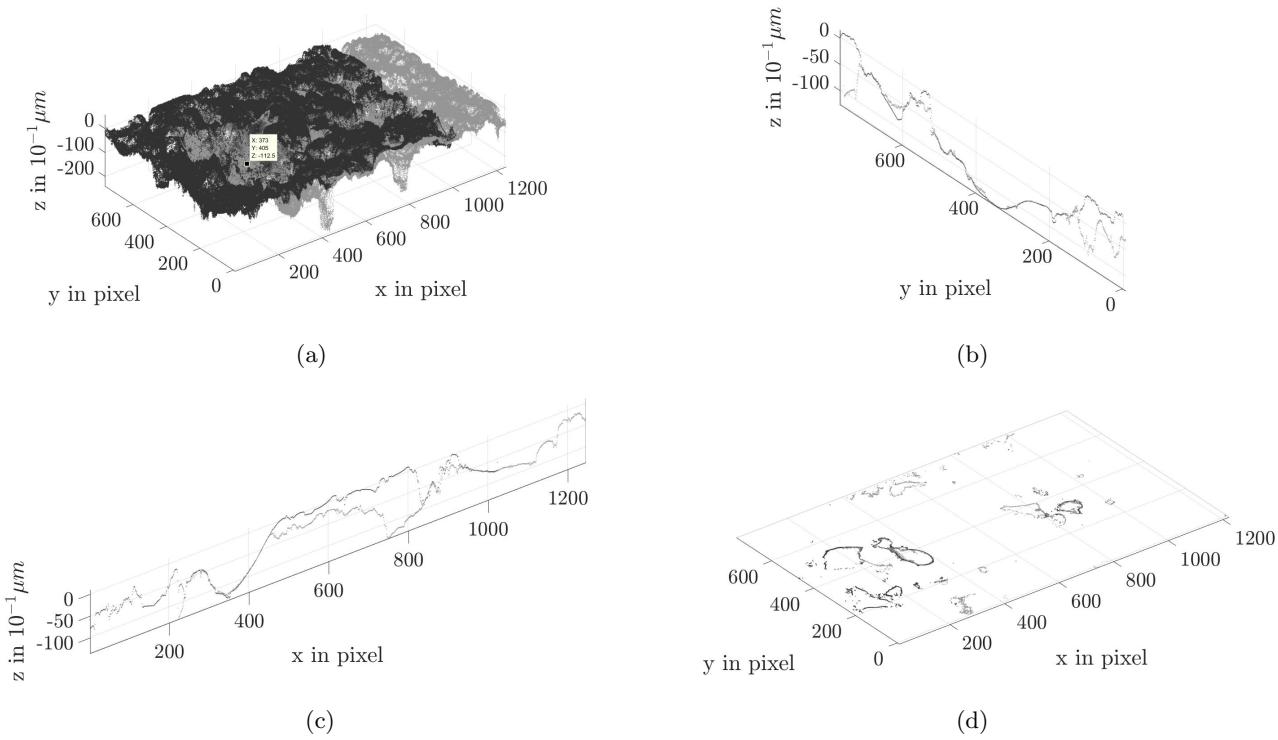

Figure 5: Two aligned pointclouds (a). Profil in y-direction at x = 373 px (b), in x-direction at y = 405 px (c) and in z-direction at z = $-11.25\mu m$ (d).

4. DISCUSSION AND CONCLUSION

The results show that a rigid 3D registration of subsequently milled coatings, implemented in a two step approach, 3D phase correlation and the TrICP, can be gained, even though the acquired topographies of the subsequent subsurfaces vary strongly due to newly arising pores or vanishing of pores. Therefore, a high resolution 3D alignment of porous surfaces is possible. The 3D phase correlation serves well even for discontinuous structures of the subsurfaces and an estimation of a coarse alignment is achieved even with initially high disalignements. The subsequent fine alignment step, implemented by the TrICP algorithm improves the registration results. However, it needs to be mentioned that the presented registration process is only valid for porous surface structure which ensures to measure at least a small portion of the microstructure after the milling process. The alignment of the data enables to study the structure beneath the surface, in our studies, e.g., embedded pores, to gain further information on the porous network. Further steps would be a reconstruction of the pore network based on the registered subsurfaces. This information is to serve a better understanding of the porous network and further allows, e.g., to measure both the open and the closed porosity independently.

5. ACKNOWLEDGMENTS

We gratefully acknowledge funding of this work by the "Dr. Jürgen und Irmgard Ulderup Stiftung".

REFERENCES

[1] Bruzzone, A., Costa, H. L., Lonardo, P. M., and Lucca, D. A., "Advances in engineered surfaces for functional performance," *CIRP Annals - Manufacturing Technology* **57**(2), 750–769 (2008).

[2] Coutelieris, F. A. and Delgado, J. M. P. Q., "Fundamentals of Porous Structures," in [*Transport Processes in Porous Media*], Coutelieris, F. A. and Delgado, J., eds., *Advanced Structured Materials* **20**, 5–21, Springer Berlin Heidelberg, Berlin, Heidelberg (2012).

[3] Drach, B., Drach, A., and Tsukrov, I., "Characterization and statistical modeling of irregular porosity in carbon/carbon composites based on X-ray microtomography data," *ZAMM - Journal of Applied Mathematics and Mechanics / Zeitschrift für Angewandte Mathematik und Mechanik* **93**(5), 346–366 (2013).

[4] Balach, J., Soldera, F., Acevedo, D. F., Mucklich, F., and Barbero, C. A., "A direct and quantitative three-dimensional reconstruction of the internal structure of disordered mesoporous carbon with tailored pore size," *Microscopy and microanalysis : the official journal of Microscopy Society of America, Microbeam Analysis Society, Microscopical Society of Canada* **19**(3), 745–750 (2013).

[5] Joos, J., Carraro, T., Weber, A., and Ivers-Tiffée, E., "Reconstruction of porous electrodes by FIB/SEM for detailed microstructure modeling," *Journal of Power Sources* **196**(17), 7302–7307 (2011).

[6] DIN Deutsches Institut für Normung e. V., "DIN ISO 25178-3 Geometrische Produktspezifikation (GPS) - Oberflächenbeschaffenheit: Flächenhaft," (November 2012).

[7] Hao, Q., [*Optische 3D-Erfassung und Auswertung technischer Oberflächen hinsichtlich ihres Verschleißverhaltens*], Berichte aus dem Institut für Mess- und Regelungstechnik der Universität Hannover, Shaker, Aachen (2011).

[8] Chetverikov, D., Svirko, D., Stepanov, D., and Krsek, P., "The Trimmed Iterative Closest Point algorithm," in [*Proceedings / 16th International Conference on Pattern Recognition*], Kasturi, R., ed., 545–548, IEEE Computer Society, Los Alamitos, Calif. (2002).

[9] Lincoln, L. and Gonzalez, R., "Dense 3D Mapping Using Volume Registration," in [*Nature of Computation and Communication: Second International Conference, ICTCC 2016, Rach Gia, Vietnam, March 17-18, 2016, Revised Selected Papers*], Vinh, P. C. and Barolli, L., eds., 22–32, Springer International Publishing, Cham (2016).

[10] Chen, Y. and Medioni, G., "Object modelling by registration of multiple range images," *Image and Vision Computing* **10**(3), 145–155 (1992).

[11] Besl, P. J. and McKay, N. D., "A method for registration of 3-D shapes," *IEEE Transactions on Pattern Analysis and Machine Intelligence* **14**(2), 239–256 (1992).

[12] Rusinkiewicz, S. and Levoy, M., "Efficient variants of the ICP algorithm," in [*Proceedings / Third International Conference on 3-D Digital Imaging and Modeling*], 145–152, IEEE Computer Soc, LosAlamitos, Calif. (2001).